American Physical Society
1963 Spring Meeting
Washington, D. C.,
April 22-25, 1963

Conf-48-112

SUPERCONDUCTIVITY IN A STRONG SPIN EXCHANGE FIELD*

Peter Fulde and Richard A. Ferrell
University of Maryland, College Park, Maryland

Department of Physics and Astronomy

Technical Report 344

December 1963

UNIVERSITY OF MARYLAND
DEPARTMENT OF PHYSICS AND ASTRONOMY
COLLEGE PARK, MARYLAND

DISCLAIMER

SUPERCONDUCTIVITY IN A STRONG SPIN EXCHANGE FIELD*

Peter Fulde and Richard A. Ferrell
University of Maryland, College Park, Maryland

Department of Physics and Astronomy

Technical Report 344

December 1963

*Research supported in part by the Air Force Office of Scientific Research and by ARPA. This work forms a portion of a thesis submitted by one of the authors (Peter Fulde) to the faculty of the University of Maryland in partial fulfillment of the requirements for the Ph.D. degree.

SUPERCONDUCTIVITY IN A STRONG SPIN-EXCHANGE FIELD*

Peter Fulde and Richard A. Ferrell
University of Maryland, College Park, Maryland

ABSTRACT

A strong exchange field, such as produced by ferromagnetically aligned impurities in a metal, will tend to polarize the conduction electron spins. If the metal is a superconductor, this will happen only if the spin-exchange field is sufficiently strong compared to the energy gap. When the field is strong enough to break many electron pairs, the self-consistent gap equation is modified and a new type of depaired superconducting ground state occurs. In the idealization of a spatially uniform exchange field with no scattering, it is found that the depaired state has a spatially dependent complex Gorkov field, corresponding to a non-zero pairing momentum in the BCS model. The presence of the "normal" electrons from the broken pairs reduces the total current to zero, gives the depaired state some spin polarization, and results in almost normal Sommerfeld specific heat and single-electron tunneling characteristics. The non-zero value of the pairing momentum also gives rise to an unusual anisotropic electrodynamic behavior of the superconductor, as well as to a degenerate ground state and low-lying collective excitations, in accordance with Goldstone's theorem. The effects of scattering in an actual superconducting ferromagnetic alloy have not been studied and may interfere with experimental investigation of the theoretical results found in this paper for the idealized model.

I. INTRODUCTION

There is experimental evidence of ferromagnetic alignment of paramagnetic impurities when they are in the form of a dilute solution, dissolved in certain non-magnetic metals. A typical example is the recently reported[1] ferromagnetism of 0.8 percent of iron dissolved in gold, which has been found to exhibit a Curie temperature of 9° Kelvin. In some cases, when the host metal becomes a superconductor at sufficiently low temperature, there is further evidence that the ferromagnetic alignment persists after the onset of superconductivity; e.g., gadolinium dissolved in lanthanum.[2,3] This situation raises the question of the nature of the perturbed state of the superconducting electrons, which are under the influence of the strong exchange field exerted on them by the ferromagnetically aligned paramagnetic impurities. The purpose of the present paper is to report a new solution to this problem, which leads to a state quite different from the conventional BCS ground state of the superconductor.[4]

According to the conventional point of view, the exchange field exerted by the ferromagnetic impurities upon the conduction electron spins is either too weak to produce a change in the BCS state, or it produces a first-order phase transition to the normal state. The strength of exchange field required to overcome the energy gap and flip the spin of a superconducting electron is $\sqrt{2}$ greater than the strength at which the phase transition occurs.[5] But we shall demonstrate that at a somewhat lower value of strength, an unexpected solution of the pairing equations enters. Thus a first-order phase transition takes place from the BCS to this new phase, the "depaired" state, which subsequently passes continuously by a second-order phase

transition into the normal state as the strength of the exchange field is increased.

The new solution can be found only by studying significant departures from the BCS solution. Such situations are studied in Section II where the gap equation is solved for the case of a relatively large number of electron pairs broken. A doubly infinite manifold of wave functions is found, depending upon the assumed mean momentum of pairing, Q, and the assumed value of the strength of exchange field, H. In Section III a singly infinite family of solutions of the gap equation is selected which represents the ground state solutions in the presence of an exchange field of varying strength H. According to Bloch's theorem,[6] in order that these solutions should represent the ground state, they should exhibit zero current. This is accomplished by balancing the total current of the unpaired electrons against the supercurrent generated by the non-zero value of pairing momentum, Q. This requirement produces a function Q(H) so that, for every assumed value of the exchange field, there is a unique value of the pairing momentum. For these zero-current solutions the magnetization is calculated and hence the free energy in the ground state. In Section IV the peculiar anisotropic electrodynamic properties resulting from the non-vanishing pairing momentum are studied. It is found that a supercurrent of the usual London type flows in response to an applied vector potential parallel to Q, but that no supercurrent results for a weak vector potential perpendicular to Q. In Section V it is demonstrated that the presence of unpaired "normal" electrons in the depaired state causes it to have a Sommerfeld specific heat and a single-electron tunneling characteristic practically indistinguishable from those of the normal state. Section VI constitutes a brief summary.

II. EFFECT OF ELECTRON DEPAIRING ON THE ENERGY GAP

Throughout this paper the actual system under consideration, namely a dilute solution of paramagnetic impurities dissolved in a metal, will be idealized by a constant exchange field independent of space which acts only upon the electron spins. If the energy of splitting of the conduction electrons in the presence of this exchange field is $2H\Delta_o$, where Δ_o is the BCS energy gap parameter, then we can write the Hamiltonian for our model in the form,

$$\mathcal{H} = \mathcal{H}_o + H\Delta_o \sum_i \sigma_i \quad , \tag{1}$$

where $\mathcal{H}_o$ is the usual Hamiltonian for a superconductor in the absence of an exchange field, and σ_i is the operator ± 1 for the i-th electron, depending upon whether it is aligned parallel ("up") or anti-parallel ("down"), respectively, relative to the exchange field. An approximate eigenfunction of the Hamiltonian of Eq. (1) is obviously the usual BCS ground state wave function, with the associated eigenvalue simply the standard BCS ground state energy. This is true because the second term in the right-hand member is proportional to the component parallel to the field of the total electron spin in the superconductor, which operator commutes with $\mathcal{H}_o$.

If we want to find other eigenfunctions of $\mathcal{H}$, we may at first try states of small total spin, corresponding to the breaking of only a few electron pairs. If the number of electron pairs broken is small enough not to affect the energy gap, then an energy of $2\Delta_o$ has to be expended for each pair broken, while the reorientation of the electron spin gains, according to Eq. (1), $2H\Delta_o$ for each pair broken. Thus, it is not possible to find a wave function of this type corresponding to an energy lower than the BCS ground state energy,

unless H is greater than unity. But it is easy to establish[5] that the normal state, because of its response to the applied exchange field, undergoes sufficient spin orientation to acquire a lower free energy than the BCS ground state already at a value of $H = 1/\sqrt{2}$. Thus, states of small spin excitation relative to the BCS ground state are necessarily excited states of the superconductor. It is nevertheless useful, in our search for alternative ground state wave functions, to consider such excited states, and to imagine that the excess spin, and hence the number of unpaired electrons, becomes continually greater. Eventually the number of unpaired electrons will be sufficiently large to affect the energy gap and to reduce it. Nevertheless we still will have some pairing taking place and some coherence energy. The gap equation of BCS will still apply in essentially its original form:

$$\Delta = V \sum_{\underset{\sim}{k}}{}' [h_{\underset{\sim}{k}}(1-h_{\underset{\sim}{k}})]^{\frac{1}{2}}$$

$$= N V \int_0^{\omega} \frac{\Delta}{E} \, d\epsilon - V \sum_{\text{excl}} \frac{\Delta}{2E_{\underset{\sim}{k}}} \quad , \tag{2}$$

where

$$E_{\underset{\sim}{k}} = (\Delta^2 + \epsilon_{\underset{\sim}{k}}^2)^{\frac{1}{2}} \quad . \tag{3}$$

The prime signifies an omission from the sum over $\underset{\sim}{k}$ space, corresponding to the blocking of states by the presence of unpaired electrons. Otherwise the standard notation of the BCS paper is followed. The effect of blocking[7] is expressed in the second term of the right-hand member of Eq. (2) where the sum over momentum space is to be carried out over all of the excluded regions of momentum space. Such regions of momentum space are prevented by the Pauli exclusion principle

from participating in the virtual pair scattering which gives rise to the energy gap Δ. Because of the blocking of these regions, we find, in the weak coupling limit $(\omega >> \Delta)$ the following suppression of the energy gap:

$$\frac{\Delta}{\Delta_o} = \exp\left\{ - \frac{1}{2N} \sum_{excl} [E_k(\Delta)]^{-1} \right\} , \tag{4}$$

where the dependence of the right-hand member upon the energy gap has been indicated explicitly. (In all of the work in this paper we restrict ourselves to the case of zero temperature.)

The most natural blocking configuration might be assumed to be one which is spherically symmetric in momentum space, corresponding to a uniform distribution of unpaired electrons of down spin at the surface of the Fermi sea. More detailed examination reveals, however, that such excess spin states are unstable and that the spherical symmetry of the blocking region can be modified, leading to a lowering of the energy of the system. As a result the unpaired electrons tend to congregate at one portion of the Fermi surface. Hence it is necessary to consider asymmetrical blocking regions. These give a net current flow for the unpaired electrons. In order to satisfy Bloch's theorem it is consequently necessary to have an equal and opposite current flow for the superconducting electron pairs. In this Section we find the solution for the general case of non-zero pairing momentum and impose the requirement of exact cancellation of current only in the next Section.

Since it is our goal to find the lowest energy eigenvalue associated with the Hamiltonian of Eq. (1), we impose the requirement on the blocking region that it be such that no elementary excitations of negative energy are possible. The quasi-particle energy associated

with the addition of a single particle of wave number $\underset{\sim}{k}$, normal energy $\varepsilon_{\underset{\sim}{k}}$, in the present model leads to an excitation energy of the usual BCS quasi-particle energy plus additional magnetic and kinetic energy terms which are such that we obtain the boundary of the blocking region by the following formula:

$$\begin{aligned} 0 &= E_{\underset{\sim}{k}} + Q\mu_{\underset{\sim}{k}}\,\Delta_o + H\,\sigma\,\Delta_o \\ &= \Delta\,[(1+\varepsilon_{\underset{\sim}{k}}^2/\Delta^2)^{\frac{1}{2}} + q\,\mu_{\underset{\sim}{k}} + h\sigma] \quad . \end{aligned} \tag{5}$$

$Q\Delta_o$ is the pairing momentum times the Fermi velocity and $\mu_{\underset{\sim}{k}}$ is the cosine of the angle between the pairing momentum and $\underset{\sim}{k}$. For convenience in the analysis, the pairing momentum has also been measured in units relative to the actual gap Δ, rather than the unperturbed gap Δ_o, resulting in the new parameters $q = Q\Delta_o/\Delta$ and $h = H\,\Delta_o/\Delta$. Such a blocking region is illustrated by the shaded portion of Fig. 1(a), which corresponds to the region of momentum space occupied with certainty by electrons of down spin. Figure 1(b) shows the region (shaded) which is completely vacant of up-spin electrons and which does not participate in the virtual pair scattering. This is because of the blocking effect of the down-spin electrons at the opposite side of the Fermi surface. As can be seen from Fig. 1 the case of vanishing normal particle energy, $\varepsilon = 0$, gives the intersection of the blocking boundary with the Fermi surface and determines the angle subtended by the blocking region,

$$\mu_{\pm} = -\,q^{-1}\,(1\pm h) \tag{6}$$

The plus and minus signs refer to the case of up- and down-spin electrons, respectively. Equation (6) applies, of course, only when the cut-off values of the cosine of the angle fall within the physical

region of $-1 \leq \mu_{\pm} \leq +1$. Figure 1 is drawn for the special case that only unpaired down-spin electrons are present $(1 \geq q-h \geq -1)$. This depairing situation involving only a single species of electron spin will be referred to as type S, while the case of $q-h < -1$ gives down-spin electrons encircling the Fermi sea and will be referred to as type E blocking. In addition to these two cases, we have the situation of double depairing, when an excess of unpaired electrons of both up- and down-spin appears at the surface of the Fermi sea. This occurs for $q-h > 1$, and will be referred to as type D depairing. This more complicated type is illustrated in Fig. 2, where it is seen that the blocking effect of the down-spin electrons is augmented by the further blocking produced by the presence of a smaller number of unpaired up-spin electrons on the same side of the Fermi surface. The ranges of the various values of pairing momentum and exchange field are shown in Fig. 3, where the stable BCS domain in the lower left-hand corner corresponds to $q+h < 1$. For $q+h > 1$ we have the three different types of depairing discussed above and occurring in the three different regions of Fig. 3 separated by the dashed lines of unit slope.

The width of the blocking region in momentum space is determined by solving for the single-particle energy from Eq. (5):

$$\frac{\varepsilon}{\Delta} = [(q\mu + h\sigma)^2 - 1]^{\frac{1}{2}} \tag{7}$$

The integration over this thin blocking region at the surface of the Fermi sphere gives the result

$$N^{-1} \sum_{\text{excl}} E^{-1} = q^{-1}[G(q+h) + G(q-h)]$$

$$= -2 \ln (\Delta/\Delta_0) \quad . \tag{8}$$

The function appearing here is defined for positive values of the argument greater than unity as

$$G(x) = x \cosh^{-1} x - (x^2-1)^{\frac{1}{2}} \quad . \tag{9}$$

For $|x| < 1$ it vanishes, while for negative values, we define $G(x)$ to be an odd function of x: $G(x) = -G(-x)$.

It is a straightforward matter to employ Eq. (8) to evaluate the gap for various assumed values of q and h. Such a calculation yields the lines of constant Δ/Δ_0 shown in Fig. 3. With the results of this calculation we can now multiply the values of q and h by Δ/Δ_0 to obtain Q and H, respectively. This transformation maps the lines of constant Δ/Δ_0 as shown in Fig. 4. These lines intercept the Cartesian axes of Figs. 3 and 4 at right angles. Equation (8) greatly simplifies along the Cartesian axes and reduces along $H = 0$ to the gap equation for large supercurrents derived by Rogers,[8] Bardeen[9] and Parmenter.[10] Along the $Q = 0$ axis, Eq. (8) reduces to the gap equation found by Sarma.[11] The present work extends these solutions away from the coordinate axes and out into the $H - Q$ plane. As exhibited in Appendix I, simplified expressions can be extracted from Eq. (8) for the behavior of the constant gap lines in the vicinity of the axes. Close to the $H = 0$ and $Q = 0$ axes these lines have the shape of parabolas which bend toward and away from the origin, respectively. The same is true in the $h - q$ diagram, as shown by the dashed lines in Fig. 3.

The points infinitely removed from the origin in Fig. 3 have been brought in Fig. 4 to the curve

$$Q + H = \frac{e}{2} \left| \frac{Q+H}{Q-H} \right|^{\frac{Q-H}{2Q}} \quad . \tag{10}$$

It is along this zero-gap line that the solutions found here by blocking pass continuously into the normal ground-state wave function. As expected for a second-order transition, it is shown in Appendix II that in the vicinity of the zero-gap line the gap is proportional to the square root of the distance in the H - Q plane from the zero-gap line. It will be noted that the region of depairing folds back upon itself along the curve

$$h = (1+4q^2)^{\frac{1}{2}} - q \quad , \tag{11}$$

labeled f in Figs. 3 and 4. In Fig. 4 this curve is an envelope of the constant gap curves and becomes a boundary for the depairing solutions in the $Q < H$ portion. The region between this folding curve and the zero-gap curve contains two depairing solutions for every value of Q and H. Thus there are two sheets of solutions, which join along the folding curve. The first of these, the "physical sheet," is contiguous to the BCS domain and is accessible by continuous variation of H and Q away from zero. On the other hand, the second, or "unphysical sheet" is inaccessible to experimental observation, as it cannot be reached by continuous variations of Q and H. It may be noted that type E blocking only gives solutions on the unphysical sheet, and in particular, that the symmetrical depairing solutions, lying along the line $Q = 0$, are a boundary of the unphysical sheet. Thus we see that they must be rejected not only because of their instability with respect to perturbations as discussed before but also because of their lack of accessibility, lying as they do on the unphysical sheet.

III. CURRENT, MAGNETIZATION, AND GROUND-STATE ENERGY

In the above section we have found a large variety of solutions to the pairing equation. Most of these correspond to some form of excited state of the system and are not of interest to us here. Our objective is to find ground-state eigenvalues of the Hamiltonian of Eq. (1). To guide us in the search for ground-state solutions, we rely upon Bloch's theorem which requires that the lowest energy solution should have zero current. Allowing for the charge-to-mass ratio of the electron, it will be convenient for us to discuss current in terms of momentum density. Therefore, we now wish to select out of all the solutions corresponding to arbitrary points in the H - Q plane of Fig. 4, those solutions which have vanishing total net momentum. But we have seen that the unpaired electrons assume an asymmetric distribution at the Fermi surface, which results in a net total momentum for them. This momentum can easily be calculated by integrating over the regions shown in Figs. 1 and 2 (allowing for the necessary factor of μ for the component of momentum in the direction of the pairing momentum) to give the following expression for the total momentum density of the unpaired or "normal" electrons:

$$P_n = -\frac{N p_F \Delta}{2q^2} \left\{ q \left[\gamma(r_+) + \gamma(r_-) \right] - \frac{2}{3} \left[\delta(r_+) + \delta(r_-) \right] \right\} , \qquad (12)$$

where $q \pm h$ has been abbreviated by $r_\pm$. The functions which have been introduced in Eq. (12) are defined as follows:

$$\gamma(x) = x\,(x^2-1)^{\frac{1}{2}} - \cosh^{-1} x \quad , \qquad (13)$$

and

$$\delta(x) = \frac{3}{2} x \gamma(x) - (x^2-1)^{3/2} \quad , \tag{14}$$

provided $x > 1$. $\gamma(x)$ and $\delta(x)$ vanish for $|x| < 1$. Besides this total momentum of the normal electrons, we have a supercurrent momentum density resulting from the common momentum of pairing, q, which gives a total value to the entire system of paired electrons of

$$P_s = \frac{2}{3} N p_F q\Delta \quad . \tag{15}$$

Bloch's theorem requires that $P = P_n + P_s$ should vanish for the ground state. This leads to the following equation for q:

$$q^3 - \frac{3}{4} q [\gamma(r_+) + \gamma(r_-)] + \frac{1}{2} [\delta(r_+) + \delta(r_-)] = 0 \tag{16}$$

In actuality, r_+ and r_- also depend upon q so that Eq. (16) is difficult to solve in the general case. For the case of $r < 1$, however, the dependence upon r_- disappears and it is possible to assign a fixed value to the variable r_+ and to solve for the corresponding value of q by the standard formula for the roots of a cubic equation. This procedure applies to the region S of Fig. 3. The solution of Eq. (16) for type D blocking is more complicated, but is facilitated by approximations which are permitted for the relatively large values of $r_\pm$ which occur for this case. The results of numerical computation are represented by the $P = 0$ curve shown in Figs. 3 and 4. Bloch's theorem is satisfied only by solutions which fall along this line. Points which fall off the line can therefore not represent ground-state energy eigenvalues of the Hamiltonian of Eq. (1). It is of interest to note that the

$Q \neq 0$ portion of the $P = 0$ curve lies entirely on the physical sheet, but that it exhibits a minimum in the $H = Q$ plane at $Q = Q_m = 0.69$ and $H = H_m = 0.63$. For field values $H < H_m$ there are no depaired solutions satisfying Bloch's theorem, and hence the BCS state is the only ground state possible.

It is of interest to locate the intersection of the $P = 0$ and $\Delta = 0$ curves. In other words, we want to find the values of the parameters Q and H at which the gap vanishes, always keeping the current zero. This is easily found from the asymptotic expressions for the functions $\gamma(r_{\pm})$ and $\delta(r_{\pm})$. The result is that the asymptotic slope in the $h - q$ plane is determined by

$$\coth (q/h) = q/h \tag{17}$$

or

$$h/q \sim 0.833 \quad . \tag{18}$$

In the $H = Q$ plane (Fig. 4) this intersection is the maximum H point along the zero gap line, as required by a simple symmetry consideration. Denoting the coordinates by Q_M and H_M, we find from combining Eq. (10) with Eq. (17) that $Q_M^2 = H_M^2 = 1/4$. Eq. (18) gives $H_M/Q_M = 0.833$, so that $(Q_M, H_M) = (0.904, 0.753)$. In the vicinity of this point, the region to the right of the zero current line corresponds to a net positive current and the region to the left, to a negative current.

Bloch's theorem is a necessary but not sufficient condition, for the lowest energy eigenvalue. It guarantees only that the energy is an extremum relative to small changes of the pairing momentum for a fixed value of field H. Thus the zero current requirement

can lead to unstable as well as stable solutions. This occurs along the boundary of the unphysical sheet ($Q = 0$ and $0.5 < H < 1.0$), as already discussed above in Section II, and also along the $0 < Q < Q_m$ portion of the $P = 0$ line. Such solutions are unstable with respect to acceleration of the supercurrent, and do not come into consideration here. It is evident from the dependence of the energy on the square of the current that all of the points lying along the $Q_m < Q < Q_M$ portion of the zero current line correspond to solutions which are locally stable. But further investigation is required to establish their actual gross stability in comparison to the other possible zero current eigenfunctions of Eq. (1), viz., the BCS state and the normal state.

For the purpose of comparing the energies of different zero current solutions it is useful, instead of summing up the various contributions to the total energy, to make use of the following differential relationship between the expectation value of the energy in a given state characterized by exchange field H, and the magnetization which is present in that state:

$$\Omega^{-1} \frac{\partial \langle \mathcal{H} \rangle}{\partial (H\Delta_o)} = -M \quad , \tag{19}$$

where Ω is the volume of the system. $\Omega^{-1}\langle \mathcal{H} \rangle$ can be identified with the free energy density F. Thus Eq. (19) is equivalent to the usual integral formula for the change in free energy upon passing between two different states, 1 and 2:

$$F_2 - F_1 = -\int_1^2 M \, d(H\Delta_o) \tag{20}$$

The magnetization is defined by the expectation value of the total component of the electron spin in the direction of the exchange field:

$$M = -\Omega^{-1} \langle \sum_i \sigma_i \rangle \tag{21}$$

With this definition of M the actual numerical value can be calculated directly by integrating over the depairing regions, with the result

$$M = \frac{N\Delta}{2q} [\gamma(r_+) - \gamma(r_-)] \quad . \tag{22}$$

This result is plotted as the curved line in Fig. 5, where the zero current line has been used to eliminate q and it will be seen that for $H_m < H < H_M$ there are two intersections of the vertical H = constant line with the magnetization curve, and hence two different magnetizations possible. These correspond to the two intersections with the zero current line in Fig. 4. As already discussed, only the upper intersection is locally stable. From Eq. (20) we see that it is also stable relative to the normal state, whose magnetization curve is the straight line passing through the origin. It remains, however, to investigate the stability of this solution relative to the BCS state. This problem is illustrated in Fig. 5 by the areas enclosed by the magnetization curve and shaded horizontally. When the value of H is such that area A is equal to area B, then, according to Maxwell's[12] rule applied to Eq. (20), the energies of the BCS and the depaired states are precisely equal. For smaller values of H the BCS state is the energetically more favorable one, while for larger values of H area B grows and area A shrinks, increasing the stability of the depaired relative to the BCS state.

The actual computation of the relative stability of the depaired state is facilitated by the knowledge that the free energies of the BCS and normal states are precisely equal at $H = 1/\sqrt{2}$. For the vertical line labeled WEAK in Fig. 5, with this value of

H, the areas A and C sum exactly to area B. For this value of H, the depaired state is more stable than both the BCS and normal states by the area C. Thus the field at which the first order transition from the BCS to the depaired phase occurs is slightly less than $1/\sqrt{2}$ and is given approximately by

$$H - \frac{1}{\sqrt{2}} \approx - \frac{1}{M(1/\sqrt{2})} \int_{1/\sqrt{2}}^{H_M} (M_n - M)\, dH \quad . \tag{23}$$

Neglecting this small difference, we expect the depaired state to be the actual ground state of the system in the range $0.71 \leq H \leq 0.76$. Over this range of stability, the square of the gap varies roughly linearly with field, as $1 - H/H_n$ (see Appendix I). This is shown in Fig. 6 by the dashed parabola and can be compared with the solid curve (labeled "WEAK") which exhibits the exact variation of Δ/Δ_o vs. H. The gap decreases from the value $0.23\ \Delta_o$ at $H = 0.71$ to zero at $H = H_M$, where it has infinite slope and the second-order transition to the normal state occurs.

The behavior of the free energy over this range is shown by the curve, labeled "WEAK", in Fig. 7, where F(in units of the BCS condensation energy) is plotted vs. H. As noted above, the magnetization in the depaired state is only slightly less than that in the normal state. Consequently, the free energy is also only slightly lower--by a few tenths of a percent of the BCS condensation energy. As we will demonstrate immediately, this is greatly increased by the exchange interaction of the normal electrons among themselves. But even without this effect, one should not suppose that the depaired state could easily be spoiled by a slight increase in temperature above absolute zero. Although the detailed temperature dependence of the model remains to be investigated (except for the $H = 0$ and

$Q = 0$ lines studied in references 9 and 11, respectively), one should expect that the magnitude of the energy gap should determine the transition temperature.

A further feature of the free energy shown in Fig. 7 is the cusp arising from the double-valued nature of M vs. H and from the infinite slope in Fig. 5 at $H = H_m$. The locally unstable depairing solutions, already rejected above, lie beyond the cusp in Fig. 7.

In the above work the interaction between a pair of electrons has been included, but the interaction of unpaired electrons neglected. The same potential which produces scattering between pairs of electrons and leads to the establishment of the energy gap will also give exchange scattering between any two normal electrons and thereby modify the energy of the depaired state. This effect decreases the stability of the depaired state relative to the BCS state, but its effect on the normal state is even greater, because of the larger magnetization. The effect of the interaction on the spin susceptibility is already well known in non-superconducting metals. For the repulsive Coulomb potential this is the usual exchange scattering which favors ferromagnetism, and for paramagnetic metals tends to increase the paramagnetic spin susceptibility. It is an effect which is included by Landau[13] in his discussion of the quasi-particle treatment of the spin susceptibility of a Fermi liquid, and has also been discussed from a somewhat different point of view by one of the present authors[14]. A useful picture for this effect is that of the molecular field, the basis of the Weiss theory of ferromagnetism. In the present case of interest, because of the attractive short-range potential of the BCS theory the molecular

field is opposite in sign relative to its usual direction and is unfavorable to the polarization of electrons[15]. It subtracts from the actual external exchange field applied to the sample, H_{ex}. Thus the net magnetic field which effectively serves to act on any given electron spin is

$$H_{eff} = H_{ex} - \frac{NV}{2}\frac{M}{N\Delta_o} \quad . \tag{24}$$

This relationship between the effective forcing field, H_{eff}, and the response to it, M, is similar to that already familiar in electronic circuitry. There the signal applied to a circuit element in series with a load impedance is reduced by the current flowing through the load, in proportion to its impedance. If the response of the circuit element is known for any value of the net effective input, then a simple construction of the "load line" on a graph of current vs. input leads to a self-consistent determination of both the net effective input and the output for any given value of applied signal[16]. In the present case, the load line is a straight line of slope $-2/NV$ drawn on Fig. 5. The intercept with the abscissa axis is H_{ex}. For any given value of the intercept, the load line is completely determined, once the value of NV has been specified for the material of interest. In the weak coupling limit, $NV \to 0$, the load line becomes the vertical line of constant applied H, already discussed in connection with Fig. 5. For stronger coupling, however, the finite slope of the load line has important consequences. First of all, it should be noticed that for a given value of H_{ex}, the normal magnetization is reduced by the factor $1 + NV$. Consequently the value of the external field at which the gap in the depaired state passes to zero is increased

by this same factor, giving

$$H_M' = (1 + NV)\, H_M \quad . \tag{25}$$

This situation is illustrated in Fig. 5 by the dashed load line. A further field strength of interest is the value for which the BCS and normal states have equal free energy. In the weak coupling limit this is $1/\sqrt{2}$. Because of the suppression of the normal state susceptibility, this field is increased by the factor $(1 + NV)^{1/2}$. The areas enclosed between the load line corresponding to this value of H_{ex} and the magnetization curve are shown with vertical shading. Areas A and C sum exactly to area B. As discussed above in connection with Eq. (23), the value of H_{ex} defined in this way is only slightly greater than the value at which the first-order phase transition occurs between the BCS and depaired states. Because of the stronger dependence of H_M' on NV, it is evident that the range of stability of the depaired state is increased by strong coupling. As a numerical illustration, $NV = 1/2$ may be chosen to represent the strongest coupling case encountered among the superconductors. This gives $H_M' = 1.13$, while the equality of the BCS and normal state free energies occurs at $H_{ex} = 0.87$. Application of Eq. (23) yields a slightly lower value for the first-order transition to the depaired state, leading to stability of the depaired state in the following range

$$0.83 < H_{ex} < 1.13 \quad . \tag{26}$$

This is a range of stability of about 30 percent. The smallest value of external field for which a depaired solution exists at all is found by shifting the load line of Fig. 5 to the left until

it becomes tangent to the magnetization curve. This yields $H_m' = 0.79$. Thus it is seen that for strong coupling the effect of exchange between the depaired electrons is to make most of the locally stable depaired solutions stable also relative to the BCS state. The range of stability covers almost the entire range of available solutions. This situation is illustrated in Fig. 7 by the curve labeled "STRONG" for which the free energy is greater than that of the BCS state only over a small vicinity close to the cusp. Figure 6 shows the decrease ("STRONG" curve) of the gap as a function of H_{ex} from $0.6\Delta_o$ to zero at H_M'. Near H_M' the parabolic variation discussed above is a good approximation (dashed curve).

IV. ELECTROMAGNETIC PROPERTIES

The response of the depaired ground state of the superconductor to an applied electromagnetic field is easily obtained as an extension of the above work if we limit our attention to the case of small perturbations. For this case we may expand the total momentum of the electrons, including both the coherent pairs and the normal electrons, as a power series in the deviation in the $H - Q$ plane from the $P = 0$ line determined in the previous section. For small perturbations we may neglect all terms in the Taylor series expansion except the first-order terms, for which the expansion reduces simply to

$$dP = \frac{\partial P}{\partial Q} dQ + \frac{\partial P}{\partial H} dH \tag{27}$$

Let Q_o be the value of the pairing momentum which identifies the zero current depaired state for some particular value of H_{ex}. Thus the infinitesimal change dQ can be written as a deviation of the pairing momentum away from its ground state value, or $Q - Q_o$. As the load line considerations which led to Eq. (24) still apply for current-carrying states, we may differentiate Eq. (24), keeping H_{ex} fixed and neglecting the subscript on H_{eff}. This gives us the following relationship between the differential changes in the pairing momentum and in the net effective exchange field:

$$dH = -\frac{V}{2\Delta_o} \frac{\partial M}{Q} dQ - \frac{V}{2\Delta_o} \frac{\partial M}{\partial H} dH \tag{28}$$

Elimination of dH from Eqs. (27) and (28) yields a simple linear relationship between $dQ = Q - Q_o$ and the current J, which is proportional to dP:

$$J = -\frac{c^2 \Delta_o}{4\pi e v_F} \lambda^{-2} (Q - Q_o) \tag{29}$$

This equation serves to define the quantity λ^{-2}. In the weak coupling limit, $dH = 0$, and λ^{-2} is simply proportional to $\partial P/\partial Q$. λ^{-2} has the dimensions of the reciprocal of the square of a penetration depth, and therefore the result of computation is plotted in Fig. 8 as the ratio of λ^{-2} to the reciprocal of the square of the London penetration depth,

$$\lambda_L^{-2} = \frac{4\pi ne^2}{mc^2} \quad . \tag{30}$$

c is the velocity of light, e and m the electron charge and mass, and n the density of conduction electrons. The curve labeled WEAK in Fig. 8 represents the result of such a computation, while the curve labeled STRONG has been determined only near the upper end point, H_M'. Exact determination of the complete curve would require the evaluation of all four of the partial derivatives occurring in Eqs. (27) and (28), which could be carried out in a straightforward manner.

Thus we see that there is a one-to-one correspondence between the value and direction of the pairing momentum Q and J, the net current which flows in the depaired superconductor. As evident in Fig. 8, the proportionality constant is reduced roughly by a factor of two compared to the superconductor in the absence of spin-exchange field, because of the response of the normal electrons. We may now ask the question, "Suppose that a uniform current J is flowing in the depaired superconductor, what will now be the effect of a perturbing vector potential?" This question can be easily answered by noting that the presence of a weak vector potential can be alternatively described by an equivalent change in the vector momentum of pairing according to

the relation

$$\delta(\underset{\sim}{Q}\Delta_o/v_F) = \frac{e}{c}\underset{\sim}{A} \quad , \tag{31}$$

where v_F is the Fermi velocity. It is convenient to resolve the perturbing vector potential into components parallel and perpendicular to the current. The parallel component $A_{||}$ leads simply to an increment of the current in the same direction, $J_{||}$, independent of the magnitude of the current which was already present:

$$J_{||} = \frac{-c}{4\pi}\lambda^{-2} A_{||} \tag{32}$$

This equation is of the same form as London's equation for the current which flows in an ordinary superconductor in response to an applied vector potential. Thus the parameter λ, introduced above, can be identified as the penetration depth for the screening of such a disturbance by the superconductor.

The response of the depaired state to the perpendicular component of the vector potential is, however, quite different. Here a small perpendicular component serves only to rotate the direction of the pairing momentum, by an angle equal to the ratio of $eA_\perp/c$ to the quantity $Q_o\Delta_o/v_F$. According to Eq. (31) a small perpendicular vector potential does not alter the magnitude of the pairing momentum, and thus serves only to produce a perpendicular component of current proportional to the angle of rotation and to the current already present:

$$J_\perp = \frac{ev_F}{c\Delta_o Q_o} J A_\perp \tag{33}$$

The relationship expressed by Eq. (33) can be more readily understood by substituting for the original current from Eq. (29), to give the

following relationship between the perturbing vector potential and the current which flows in response to it:

$$J_{\perp} = \frac{c}{4\pi} \frac{Q-Q_o}{Q_o} \lambda^{-2} A_{\perp} \qquad (34)$$

This is similar to the relationship discussed above for Eq. (32), except now that the penetration depth is clearly current dependent, and is given by the expression

$$\lambda_{\perp} = \left(\frac{Q_o}{Q-Q_o}\right)^{1/2} \lambda \quad , \qquad (35)$$

where the quantity $Q-Q_o$ can be expressed in terms of J if preferred. It will be noted that only positive values of $Q-Q_o$ give stability of the system with respect to perpendicular disturbances (instability is formally expressed by an imaginary value for the penetration depth). It should further be noted that as the current flowing through the sample is allowed to become vanishingly small, the screening of the perpendicular component of the vector potential becomes progressively weaker, and corresponds to a penetration depth which approaches infinity. It is important to keep in mind, however, that this conclusion holds only for small perturbations and that the electrodynamic properties are considerably more complicated if this restriction is not satisfied.

V. QUASI-PARTICLE SPECTRUM

The energy required to add an electron to the depaired state is easily calculated along the lines explained in the BCS paper. In the present problem special attention must be paid to the Pauli exclusion principle, which prevents the addition of a particle to a momentum state in the blocking region. On the other hand we get two types of excitation when we add an electron to one of the vacant regions in Figs. 1 or 2. These correspond to the production of a bound pair or of an excited pair. Paying attention to such details, one readily establishes that for every momentum $\underset{\sim}{k}$, there exists a quasi-particle excitation of energy given by the absolute value of the right-hand member of Eq. (5). The depaired state clearly has arbitrarily low-lying quasi-particle excitations, as is seen from the fact that along the boundary of the blocking region, Eq. (5) holds. For a given value of $\mu_{\underset{\sim}{k}}$, Fig. 9 illustrates the relationship between the BCS quasi-particle energy $E_{\underset{\sim}{k}}$ and the actual quasi-particle excitation energies, $E_{\downarrow}$ and $E_{\uparrow}$, associated with the addition of a down-spin electron of momentum $\underset{\sim}{k}$ and an up-spin electron of momentum $-\underset{\sim}{k}$, respectively. It will be noted that this is the usual relationship of the BCS theory except for a shift in the zero of energy, as shown by the solid line drawn across the graph at the positive energy $(H-\mu Q)\Delta_o$. The energy for the addition of a down-spin electron is measured upwards from this value, while the energy for the addition of an up-spin electron is measured down from this value. Differentiation of these curves with respect to E for a fixed value of μ gives the customary BCS density of state variation shown in Fig. 10, but again with a shifted energy origin. The density of states for

down-spin additions is shown to the right of the heavy vertical line, while up-spin excitations have the density of states per unit energy shown to the left of the heavy vertical line. All of the excitations are of course positive energy, as already guaranteed by the condition introduced in Section II that no negative energy excitations should be possible in the depaired ground state. The actual total density of states for the addition of a particle to the depaired state is found by superposing the portion of Fig. 10 to the right and left of the heavy vertical line and integrating over all the values of μ. This has been done for a few special cases. Figure 11 shows the density of states curve for $H = 0.64$, $Q = 0.75$, $\Delta = 0.50\ \Delta_o$, a case attainable with strong coupling near the lower end of the stability range. It will be noted that the density of states is qualitatively quite similar to the constant density of states exhibited by a normal conductor, although some structure is in evidence in Fig. 11. For stronger exchange fields, the structure is less pronounced and the density of states curve passes continuously into the constant normal density of states (dashed line in Fig. 11) as the gap decreases.

It follows from the existence of low-lying quasi-particle excitations that the depaired state should exhibit a Sommerfeld type specific heat linear in temperature. The Sommerfeld γ for the depaired state is proportional to the zero-energy value of the density of states curve for quasi-particle excitations. For the case shown in Fig. 11, this is only fourteen percent below the normal value, and approaches the normal value rapidly as the gap decreases. Normal state behavior in tunneling and in the specific heat can be expected generally to set in whenever a mechanism exists in a superconductor for breaking the electron pairs. The specific mechanism

studied in this paper, that of a uniform spin-exchange field, is by no means the only possible one. The opposite situation to that studied here, that of randomly oriented and distributed impurity spins, has been investigated by Abrikosov and Gor'kov[17]--with somewhat similar results. They found that at an impurity concentration of ninety percent of that required to reduce the gap to zero, new properties appear because of the presence of normal electrons. Normal tunneling behavior of the expected sort has been observed by Reif and Woolf[18] for various dilute solutions (e.g., iron in indium), but it is not known whether or not their ferromagnetic impurities are ordered. If not, then the Abrikosov-Gorkov theory would seem to apply, but if they are ordered, the approach developed in this paper might be more relevant.

VI. SUMMARY

The problem of a strong exchange field acting on the electron spins in a superconductor has been studied in the ideal case of a uniform field in the absence of scattering processes. It has been found that a qualitatively new depaired state with unusual properties exists over a finite range of the strength of the exchange field. As the exchange field increases, the energy gap of the depaired state decreases and passes continuously to the normal state. In contrast to the completely paired BCS state, the depaired state exhibits spin magnetization, almost normal tunneling and specific heat, and an absence of supercurrent for weak vector potentials perpendicular to the pairing momentum. It is this last feature which is the most striking and which can be expected to be the most difficult to observe experimentally. This is because scattering in an actual sample will tend to invalidate the above treatment based on plane wave single-particle states, insofar as the momentum relaxation rate in the normal state is greater than the energy gap. For short mean free path, all anisotropy in momentum space should vanish, and the effect of the uniform exchange field can be expected to be quite different from that found above. Taking into account momentum and spin relaxation in the present model remains a problem for the future.

It is interesting to note that the idealized model studied above yields a highly degenerate ground state, characterized by the direction of the pairing momentum, or alternatively, by the wave number of the sinusoidal spatial dependence of the Gorkov function. Goldstone's theorem[19] requires that there must exist low-lying collective excitations of the system. The nature of these in the present

model has not been investigated. It should also be noted that the perturbing field acting upon the superconducting electron spins in the model treated above can be an ordinary magnetic field rather than an exchange field, provided that the orbital effects of the magnetic field can be neglected. Thus, the results found here extend somewhat the high-field limit of superconductivity discussed by Clogston[15]. Similarly, the temperature dependence of the model (which has not yet been studied) might be relevant to the high-field effects investigated in tin by Knight and Androes[20].

APPENDIX I. SIMPLIFIED GAP EQUATION

Equation (8) determines the energy gap Δ for any choice of q and h, corresponding to an arbitrary point in the h - q plane. It is useful to note, however, that considerable simplification results when one of the variables is small, corresponding to the two strips in the quarter plane along the two axes. To find the dependence of the gap to second order in the small quantity, we will need the first three derivatives of the function $G(x)$, defined by Eq. (9). These are

$$G'(x) = \cosh^{-1} x \quad , \tag{36}$$

$$G''(x) = (x^2-1)^{-1/2} \quad , \tag{37}$$

$$G'''(x) = -x(x^2-1)^{-3/2} \quad , \tag{38}$$

assuming $x > 1$. Taylor's series expansions in powers of h and q are immediately found to be,

$$-2q \ln\left(\frac{\Delta}{\Delta_o}\right) = 2G(q) + h^2(q^2-1)^{-1/2} \quad , \tag{39}$$

and

$$-2q \ln\left(\frac{\Delta}{\Delta_o}\right) = 2\cosh^{-1} h - \frac{1}{3} q^2 h(h^2-1)^{-3/2} \quad , \tag{40}$$

respectively. Thus, small excursions from the $h = 0$ axis reduce the gap while small deviations from the $q = 0$ axis increase it. (The mapping into the H·Q plane shown in Fig. 4 changes, however, this last feature.) For $h = 0$, Eq. (39) becomes

$$\frac{\Delta}{\Delta_o} = \exp[-G(q)/q] \quad , \tag{41}$$

the gap equation for large supercurrents derived by Rogers[8], Bardeen[9], and Parmenter[10]. For $q = 0$, Eq. (40) can be further simplified to

$$\frac{\Delta_o}{\Delta} = h + (h^2-1)^{1/2} \quad , \tag{42}$$

and

$$\frac{\Delta}{\Delta_o} = (2H-1)^{1/2} \quad , \tag{43}$$

for $0.5 \leq H \leq 1.0$[11] as found by Sarma[11] for zero temperature.

The behavior of the constant gap curves in the h - q plane is readily obtained from Eqs. (39) and (40). Let the gap = Δ curve cut the axes at q_Δ and h_Δ. Substituting Eq. (41) (written now in terms of q_Δ) into Eq. (39) yields

$$q - q_\Delta = -\frac{q_\Delta}{2(q_\Delta^2-1)} h^2 \quad , \tag{44}$$

a parabola normal to the $h = 0$ axis and curved toward the $q = 0$ axis. Similarly, substitution of Eq. (42) (with h written as h_Δ) gives

$$h - h_\Delta = \frac{h_\Delta}{6(h_\Delta^2-1)} q^2 \quad , \tag{45}$$

a parabola normal to the $q = 0$ axis and curved away from the $h = 0$ axis. These parabolas are shown as dashed curves in Fig. 3. As the mapping of Fig. 3 onto Fig. 4 is simply a change of scale by Δ/Δ_o, the behavior of the constant gap lines in the vicinity of the $H = 0$ and $Q = 0$ axes is also that of parabolas.

APPENDIX II. SECOND ORDER PHASE TRANSITION

It is of interest to study the manner in which the energy gap vanishes as the zero gap line, Eq. (10), is approached in Fig. 4. Insertion of the asymptotic expression for $G(x)$ for large values of x into Eq. (8) gives

$$\ell n \frac{\Delta_o}{\Delta} \cong \frac{1}{2} \ell n\, 4|q^2-h^2| + \frac{h}{2q} \ell n \frac{q+h}{|q-h|} - 1 + \frac{1}{4} \frac{1}{q^2-h^2} \tag{46}$$

and

$$\left(\frac{\Delta}{\Delta_o}\right)^2 = 4(Q^2-H^2)\, \mathcal{Y}\,(Q,H) \quad , \tag{47}$$

where

$$\mathcal{Y}(Q,H) = 1 - \frac{1}{2} \ell n\, 4|Q^2-H^2| - \frac{H}{2Q} \ell n \frac{Q+H}{|Q-H|} \quad . \tag{48}$$

As setting $\mathcal{Y} = 0$ gives Eq. (10), we can write

$$|\mathcal{Y}| \cong \Delta H \left|\frac{\partial \mathcal{Y}}{\partial H}\right| = \frac{\Delta H}{H} \left(1 - \frac{1}{2} \ell n\, 4|Q^2-H^2|\right) \tag{49}$$

where ΔH is the vertical distance from the zero-gap line in Fig. 4. Substituted into Eq. (47), this gives the linear variation of the square of the gap with ΔH in the vicinity of the phase boundary. At the intersection of the zero current and zero gap lines, $4(Q^2-H^2) = 1$, so that Eqs. (49) and (47) reduce to

$$\frac{\Delta}{\Delta_o} = \left(\frac{\Delta H}{H_M}\right)^{1/2} \quad , \tag{50}$$

as already stated in the text, and as shown by the dashed parabolas in Fig. 6.

REFERENCES

*Research supported in part by the Air Force Office of Scientific Research and by ARPA. This work forms a portion of a thesis submitted by one of the authors (Peter Fulde) to the faculty of the University of Maryland in partial fulfillment of the requirements for the Ph.D. degree.

[1]R. J. Borg, R. Booth, and C. E. Violet, Phys. Rev. Letters 11, 465 (1963).

[2]B. T. Matthias, H. Suhl, and E. Corenzwit, Phys. Rev. Letters 1, 92 (1958).

[3]N. E. Phillips and B. T. Matthias, Phys. Rev. 121, 105 (1961); see also B. T. Matthias, IBM 6, 250 (1962).

[4]J. Bardeen, L. N. Cooper, and J. R. Schrieffer, Phys. Rev. 108, 1175 (1957).

[5]H. Suhl, "Low Temperature Physics," Les Houches (1961) Gordon and Breach, p. 235; edited by DeWitt, Dreyfus, and DeGennes.

[6]C. Kittel, Solid State Physics, Appendix, John Wiley and Sons (1953).

[7]The blocking effect has received some attention in the case of pairing in nuclei. See, for example, S. G. Nilsson and O. Prior, Kgl. Danske Videnskab. Selskab, Mat-fys. Medd. 32, No. 16 (1961).

[8]K. T. Rogers, Ph.D. thesis, University of Illinois, 1960 (unpublished).

[9]J. Bardeen, Revs. Mod. Phys. 34, 667 (1962).

[10]R. H. Parmenter, RCA Rev. 26, 323 (1962).

[11]G. Sarma, J. Phys. Chem. Solids 24, 1029 (1963).

[12]James Clerk Maxwell, Nature, p. 357, Vol. XI (1875); Collected Works 2, p. 425, Dover Publications.

[13]L. D. Landau, J. Exptl. Theoret. Phys. (U.S.S.R.) 30, 1058 (1956); English translation: Soviet Physics JETP 3, 920 (1957).

[14]J. J. Quinn and R. A. Ferrell, Plasma Physics 2, 18 (1961).

[15]A. M. Clogston, Phys. Rev. Letters 9, 266 (1962).

[16]This idea has also been applied by the authors to the determination of the supercurrent flowing in a doubly connected superconducting film, in response to an externally applied flux [P. Fulde and R. A. Ferrell, Phys. Rev. 131, 2459 (1963)].

[17]A. A. Abrikosov and L. P. Gor'kov, J. Expt. Theoret. Phys. (U.S.S.R.) 39, 1781 (1960) [translation: Soviet Phys.--JETP 12, 1243 (1961)].

[18]F. Reif and M. A. Woolf, Phys. Rev. Letters 9, 315 (1962).

[19]J. Goldstone, Nuovo Cimento 19, 154 (1961). See also J. Goldstone, A. Salam and S. Weinberg, Phys. Rev. 127, 965 (1962).

[20]G. M. Androes and W. D. Knight, Phys. Rev. 121, 779 (1961).

FIGURE CAPTIONS

Figure 1. Type S (single) depairing in momentum space produced by the spin-exchange field and by the shift of the Fermi sphere to the right. The heavily shaded portion of Fig. 1(a) is occupied with certainty by down-spin electrons which are stabilized by the exchange field. The Galilean transformation causes them to assume an asymmetric distribution at the Fermi surface. The shaded portion of Fig. 1(b) is completely vacant of up-spin electrons. The remaining regions of the regions are available for pairing. But because of the reduction in phase space, the energy gap is decreased.

Figure 2. Type D (double) depairing in momentum space. Here the shift of the Fermi sphere to the right is sufficiently greater than that in Fig. 1 that unpaired up-spin electrons are also stabilized, as shown by the heavily shaded region of Fig. 2(b). This requires a corresponding completely vacant region for down-spin electrons (lightly shaded in Fig. 2(a)). The residual phase space for pairing is less than in Fig. 1, giving a further decrease in the energy gap.

Figure 3. Contours of equal energy gap Δ for an ideal BCS superconductor subjected to a strong spin-exchange field h, measured in units of the gap. Δ_o is the unperturbed BCS gap for h = 0, q is the pairing momentum (i.e., shift of the Fermi sphere shown in Figs. 1 and 2), in units of the gap divided by the Fermi velocity. Regions of type E (encircling), type S (single--see Fig. 1), and type D (double--see Fig. 2) depairing are separated by the dashed straight lines. The folding line f separates the unphysical (above) from the physical (below) regions and maps into the boundary in Fig. 4. The zero-current line, P = 0, corresponds to solutions of the gap equation for which the total momentum of the unpaired electrons cancels that of the pairs. The dashed parabolas represent the approximate gap expressions derived in Appendix I.

Figure 4. Contours of equal energy gap Δ for an ideal BCS superconductor subjected to a strong spin-exchange field H, measured in units of the zero-field gap Δ_o. $Q = (\Delta/\Delta_o)q$, so that this is a mapping of Fig. 3 in which the distance of every point from the origin of Fig. 3 is reduced by the factor Δ/Δ_o. The unphysical sheet is shown shaded and joins the underlying physical sheet only along the folding

boundary f. Points infinitely distant in Fig. 3 are mapped into the zero-gap line, $\Delta/\Delta_o = 0$, a portion of which forms a boundary of the unphysical sheet. The spherically symmetric depaired solutions ($Q = 0$) also constitute a boundary of the unphysical sheet. The zero-current line, $P = 0$, lies entirely on the physical sheet and makes a normal intersection with the zero-gap line at its point of maximum H ($H_M = 0.755$). Its local stability portions are above the points W and S for weak and strong coupling, respectively.

Figure 5. Magnetization of the zero-current depaired states in units of $N\Delta_o$ (density of states times zero-field gap) vs. H (spin-exchange field in units of Δ_o). $M = 0$ in the BCS state, while the straight line (n) gives the normal state magnetization. The effect of H upon the free energy is proportional to the area under the magnetization curve. For the vertical line of Fig. 5(a) at $H = 1/\sqrt{2}$ the normal and BCS free energies are equal for weak coupling. The depaired state has lower free energy and is stable for all higher fields less than $H_M = 0.755$. See text for discussion of the slanting load lines of Fig. 5(b) pertaining to strong coupling.

Figure 6. Energy gap vs. spin-exchange field, in units of the zero-field gap, for weak and strong coupling. Exchange between the polarized electrons is unfavorable to the normal state and gives a depaired state stability range of thirty percent for strong coupling. The stability range for weak coupling is only eight percent. The dashed parabolas represent the approximate gap expression derived in Appendix II. The vertical lines with arrows indicate the first-order phase transitions which occur from the BCS to the depaired state for weak and for strong coupling.

Figure 7. Free energy F relative to zero-field normal state, in units of the BCS condensation energy E_{BCS}, for weak and strong coupling. H_{ex} is the external spin-exchange field applied to the electrons. The BCS state has no field dependence, while the normal state dependence is shown by the dashed parabolas (labeled n). The stability of the depaired state is only a fraction of a percent of E_{BCS}, but is increased by an order of magnitude by strong coupling. The second-order phase transition at the upper field (H_M and H_M^*) is represented by the tangency of the solid and dashed curves.

Figure 8. Ratio of the strengths of the London supercurrent in the depaired and BCS states vs. spin-exchange field. λ_L is the London penetration depth and λ the penetration depth for a weak vector potential applied parallel to the pairing momentum. Only the upper portion of the strong coupling curve has been determined exactly. The vertical lines with arrows indicate the first-order phase transitions which occur from the BCS to the depaired state for weak and for strong coupling.

Figure 9. Quasi-particle energies in the depaired state E vs. normal state single-electron energy ε. The zero-energy reference level for the usual BCS curve has been shifted by the energy $E_o = \Delta_o (H-\mu Q)$ to the heavy horizontal line. $\Delta_o H$ is the spin-exchange energy, $\Delta_o Q$ the pairing momentum times Fermi velocity, and Δ_o the BCS energy gap. μ is the cosine of the angle between the pairing momentum and single-particle momentum, while Δ is the actual gap in the depaired state. The energies required to add a down-spin $(E_\downarrow = E - E_o)$ or up-spin $(E_\uparrow = E_o - E)$ electron are given by the distances from the line $E = E_o$ up or down, respectively, to the hyperbola. The intersections of this line with the hyperbola determine the zero-energy quasi-particle excitations of the system.

Figure 10. Density of states per unit energy for the quasi-particle excitations formed by adding a down-spin ($E_{\downarrow} = E - E_o > 0$) or an up-spin ($E_{\uparrow} = E_o - E > 0$) electron to the depaired state, for a particular portion of the fermi sphere. Notation is the same as in Fig. 9. The state density for zero excitation energy is given by the intersection of the heavy vertical line at $E = E_o$ with the BCS curve.

Figure 11. Total density of states per unit energy vs. quasi-particle energy $E_{Q.P.}$ in units of the zero-field gap Δ_o, for the depaired state with energy gap $0.5\ \Delta_o$. The density of states shown in Fig. 10 has been summed over both spins and over all portions of the Fermi sphere. The dashed line represents the normal density of states. The structure in the depaired state, which would be observable in tunneling experiments, disappears as the exchange field is increased and the gap decreases. Because of the density of low-lying quasi-particle states, the depaired superconducting state exhibits a Sommerfeld specific heat almost as large as in the normal state. The calculation assumes that the tunneling matrix element does not depend upon the direction of the quasi-particle momentum (diffuse surface condition).

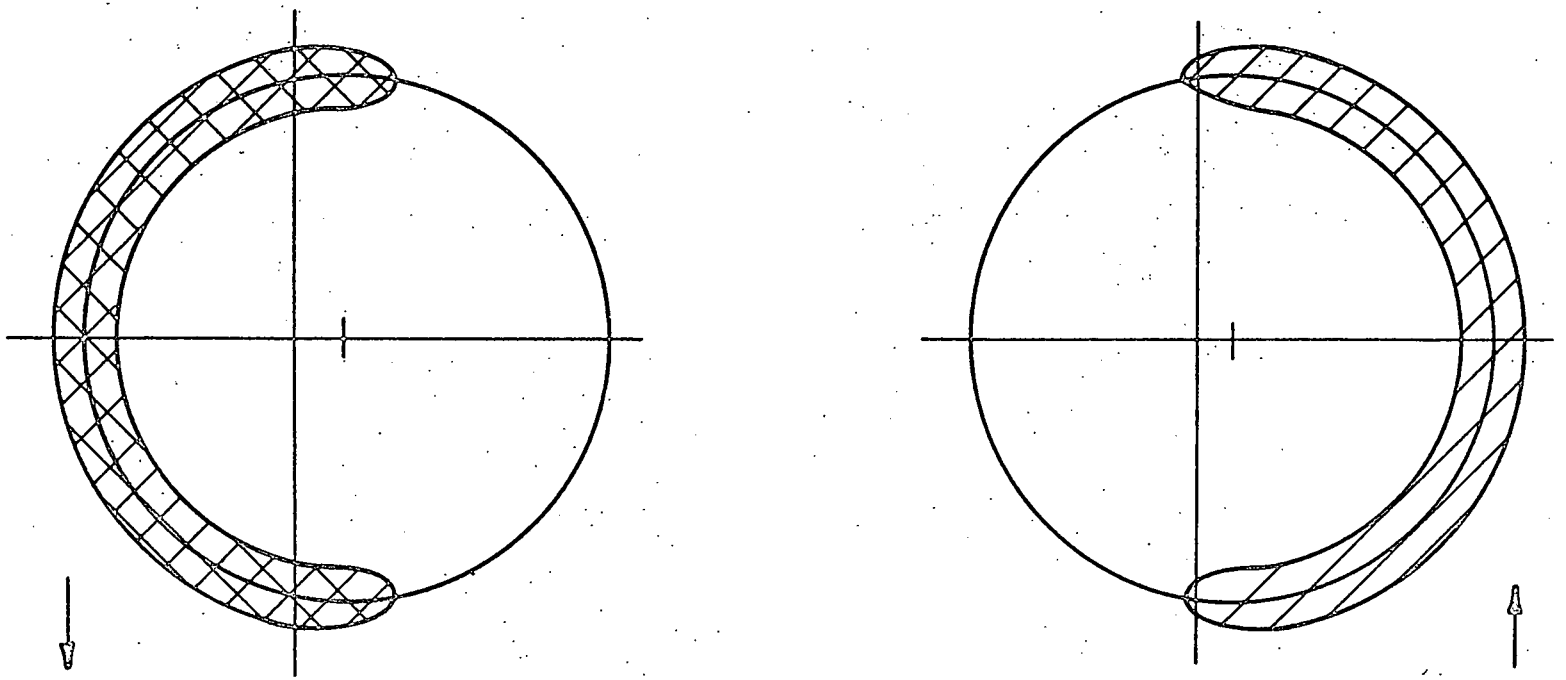

FIG. 1

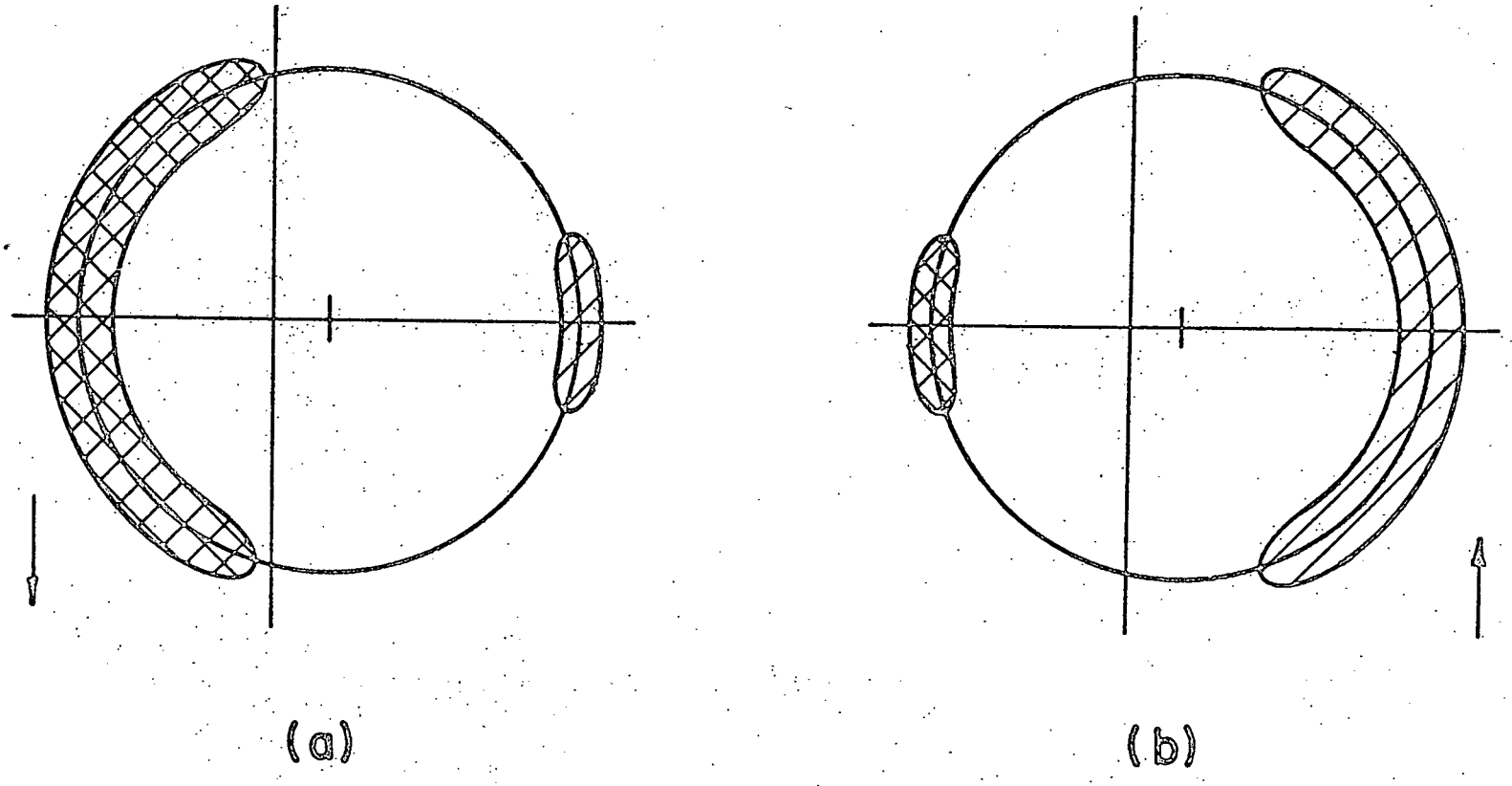

FIG. 2

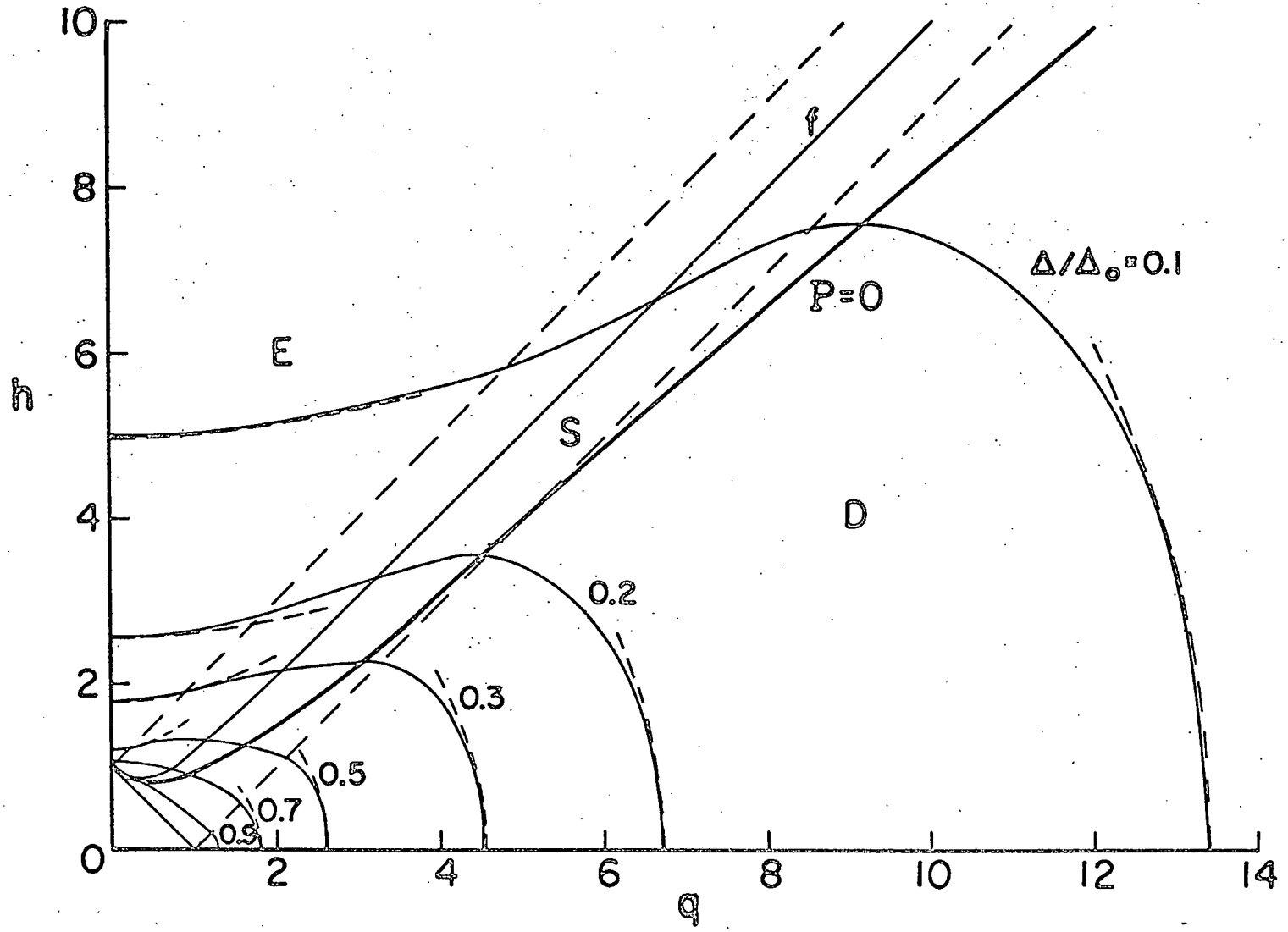

FIG. 3

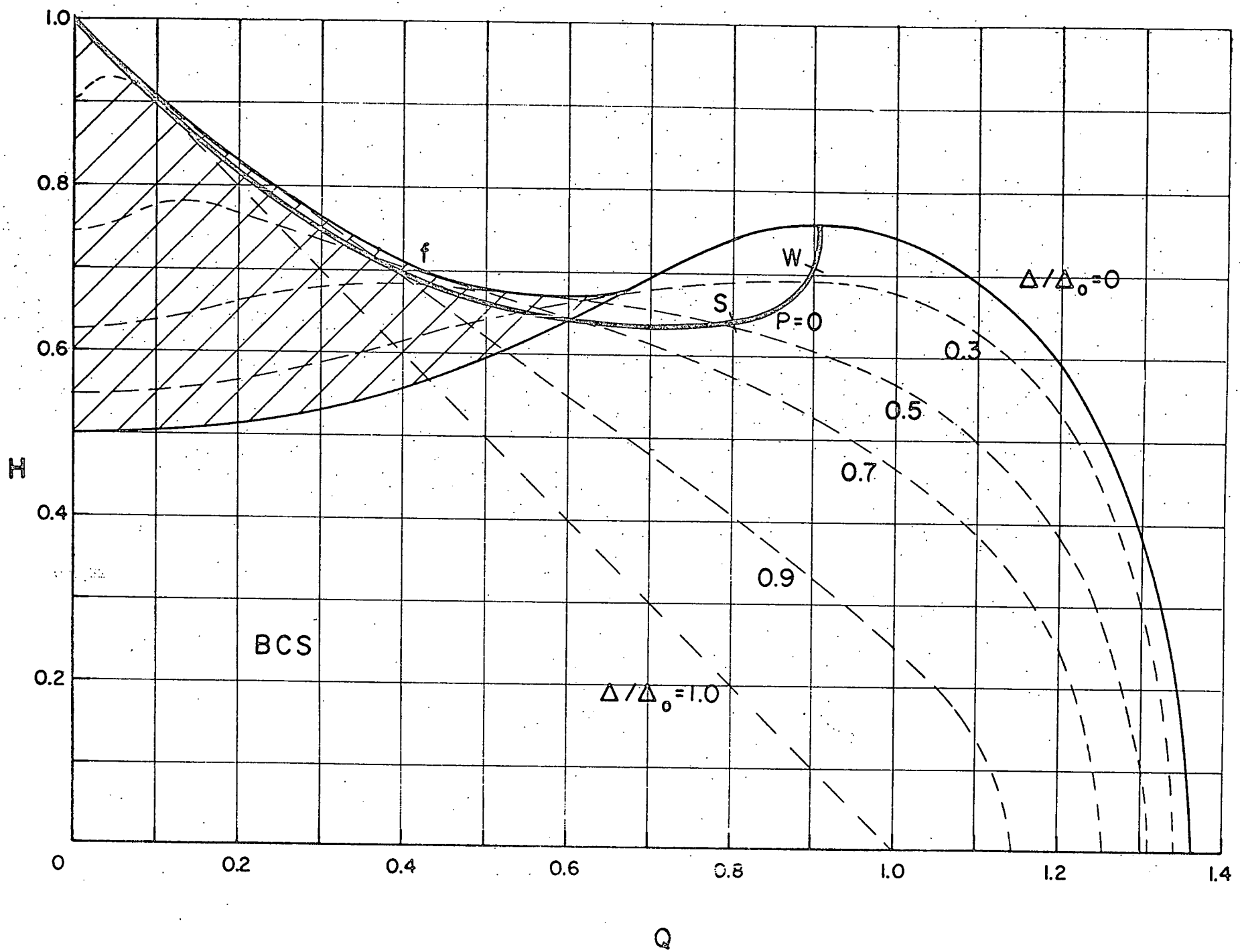
1.0
0.8
0.6
0.4
0.2
0
H
0.2
0.4
0.6
0.8
1.0
1.2
1.4
Q
f
W
S
P=0
Δ/Δ0=0
0.3
0.5
0.7
0.9
BCS
Δ/Δ0=1.0

FIG. 4

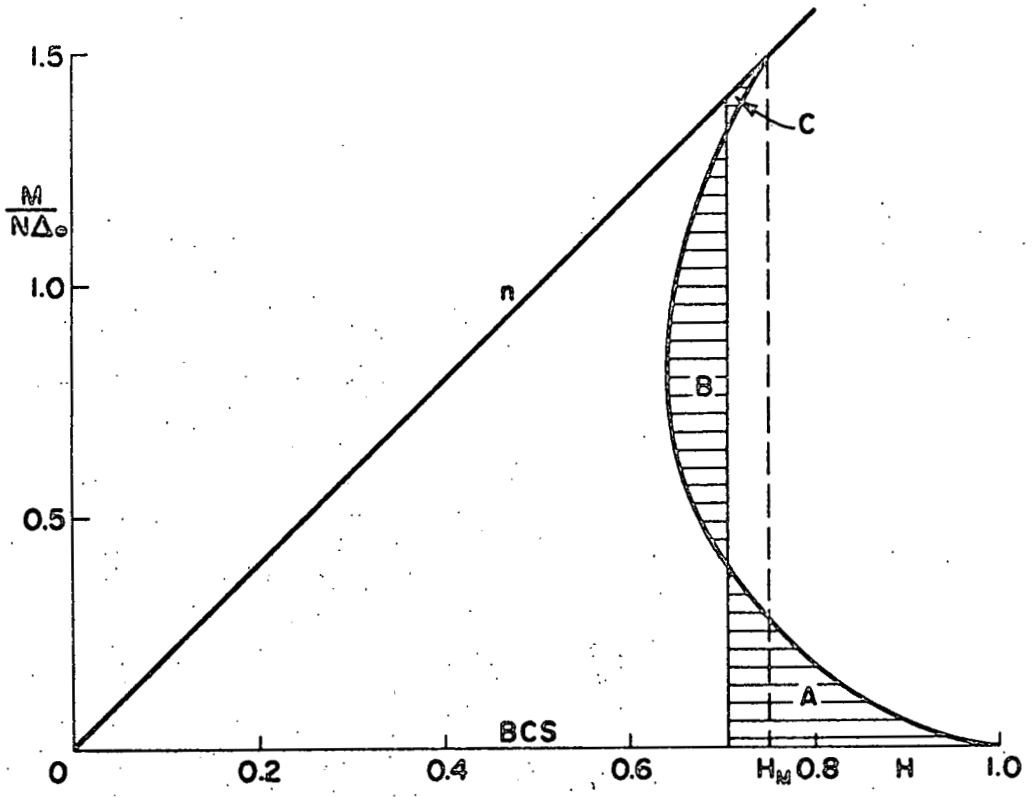

(a) WEAK

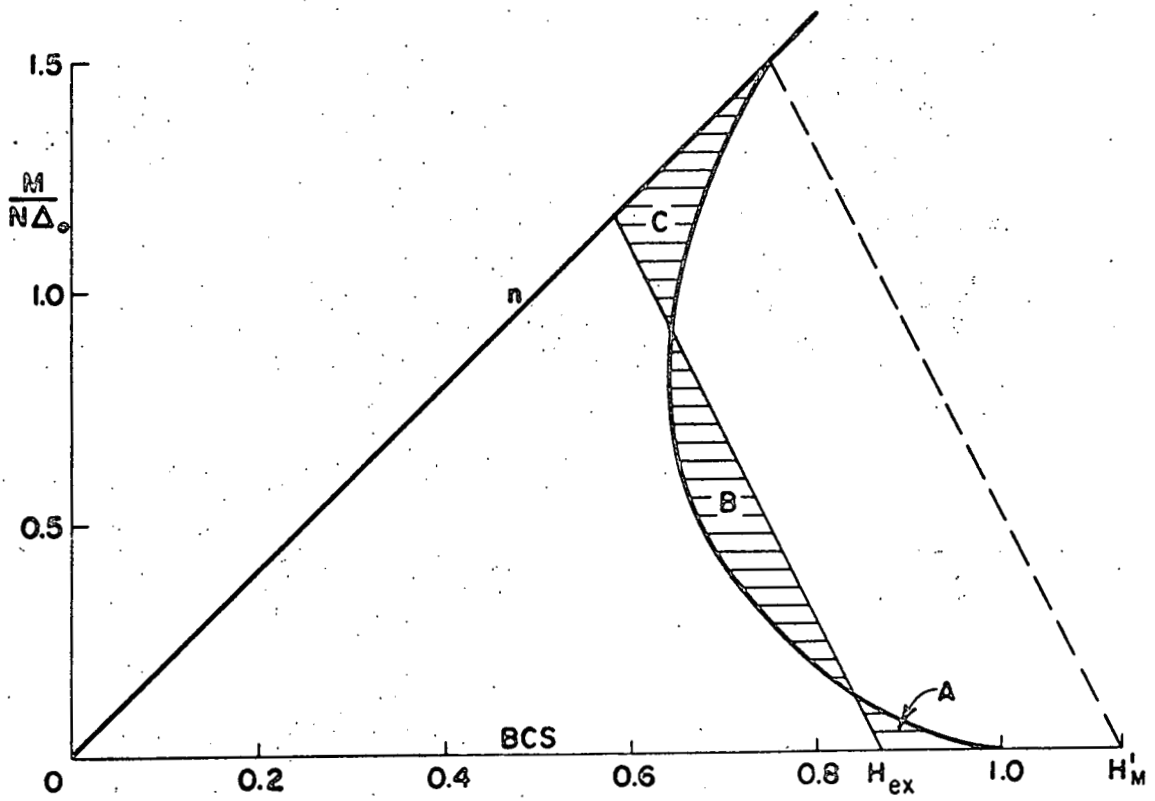

(b) STRONG

FIG. 5

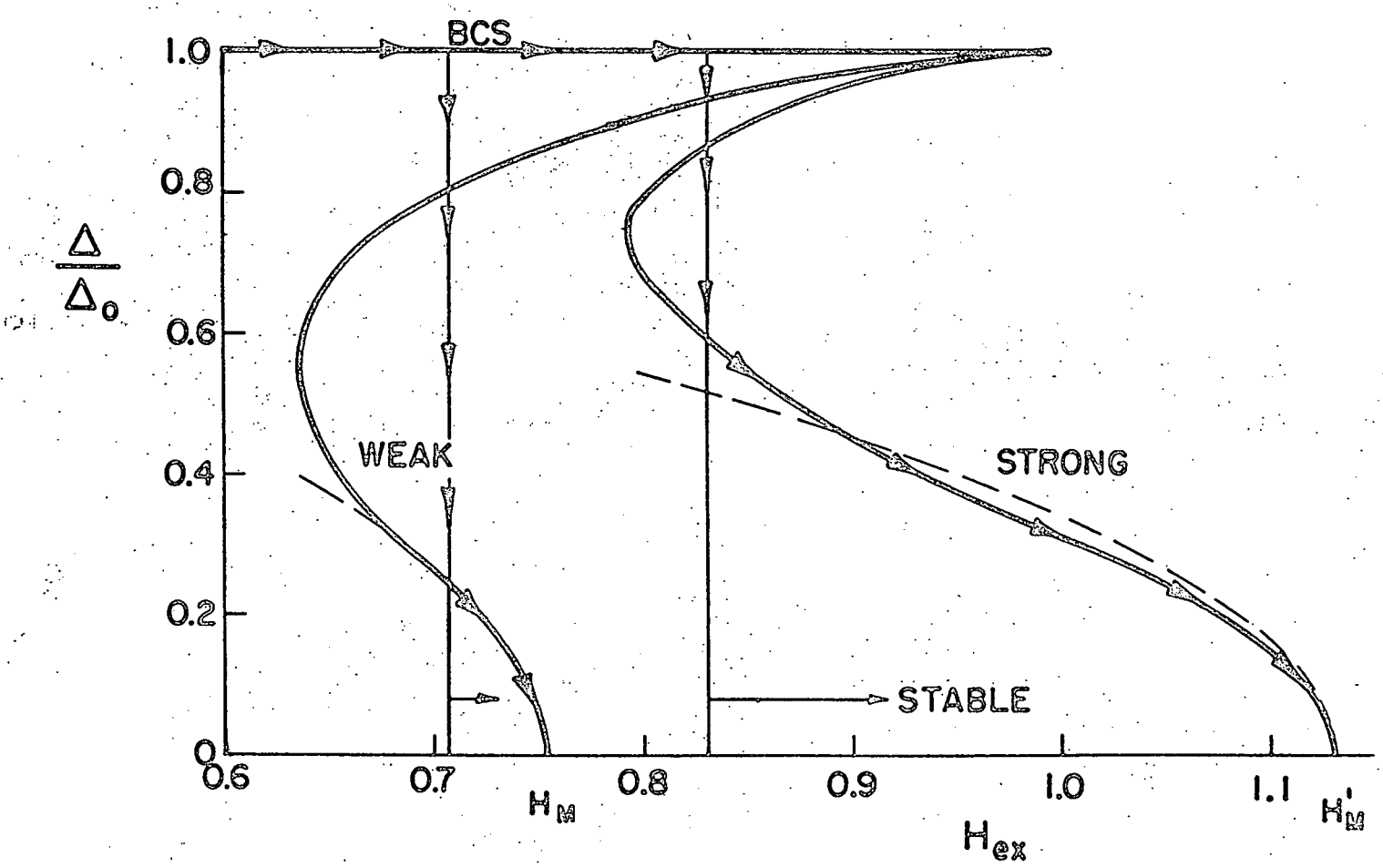
BCS
1.0
0.8
0.6
0.4
0.2
0
Δ/Δ0
WEAK
STRONG
STABLE
0.6
0.7
0.8
0.9
1.0
1.1
HM
H'M
Hex

FIG. 6

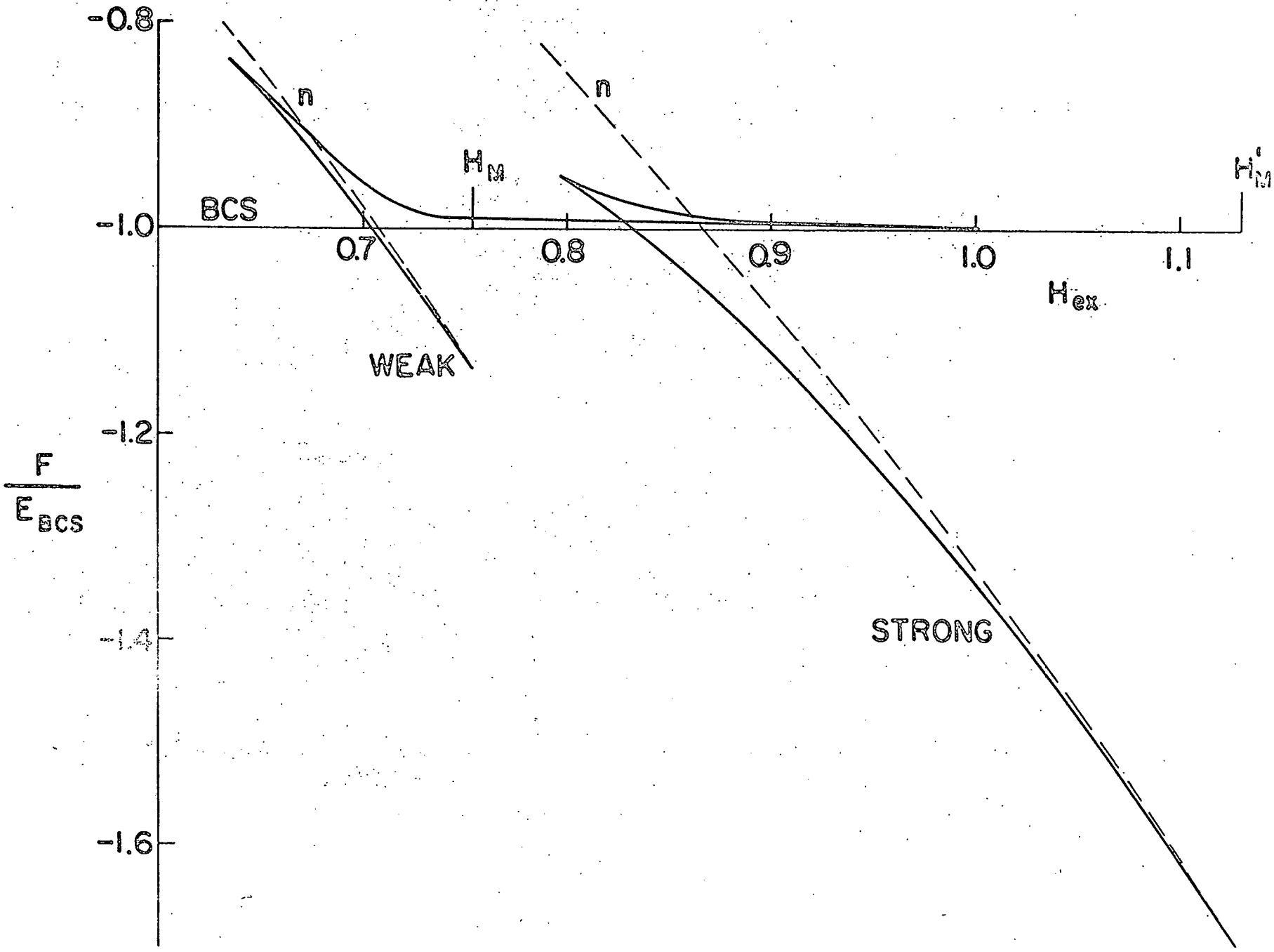

FIG. 7

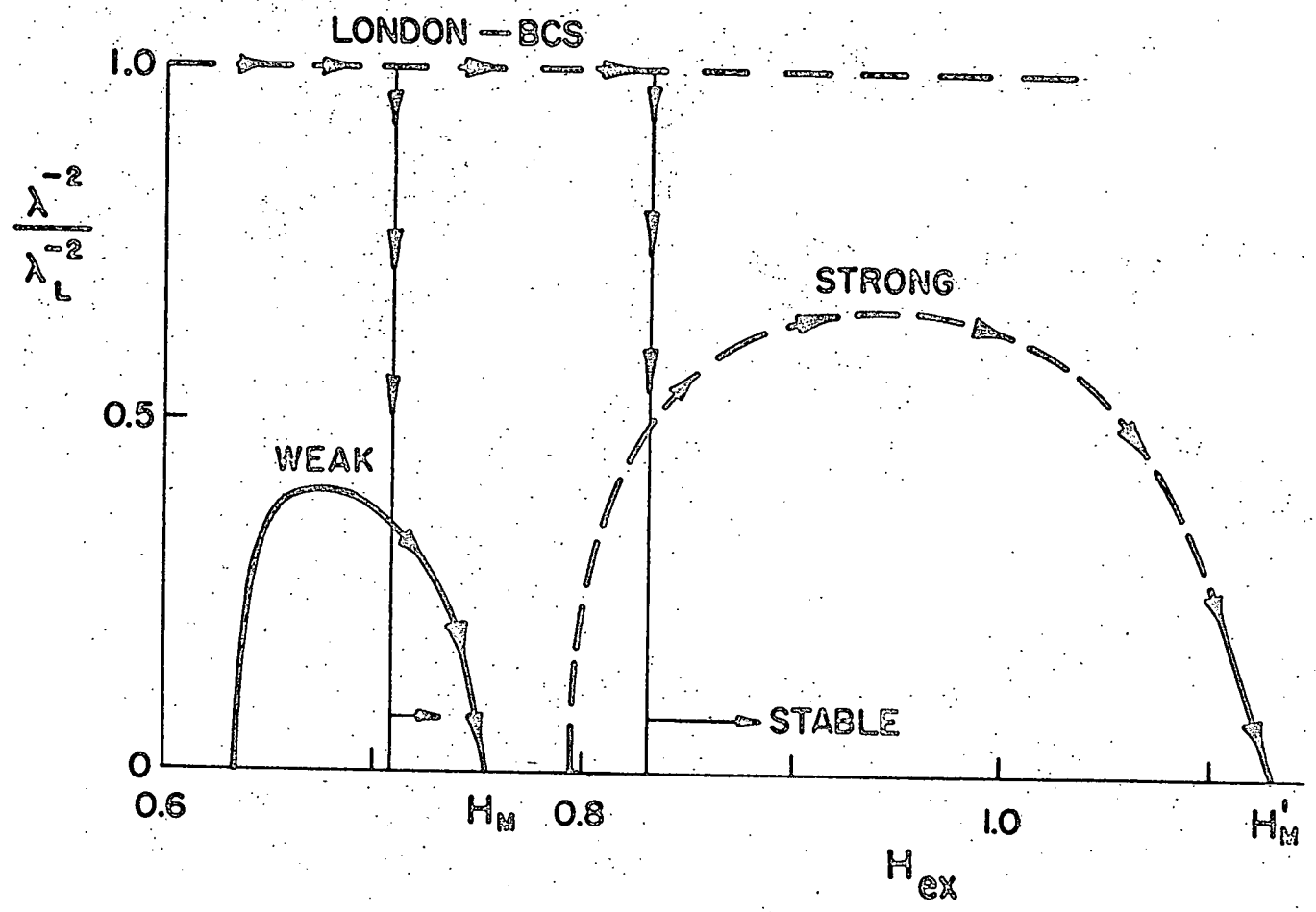
LONDON — BCS
1.0
$\frac{\lambda^{-2}}{\lambda_L^{-2}}$
0.5
0
STRONG
WEAK
STABLE
0.6
H_M
0.8
1.0
H'_M
H_{ex}

FIG. 8

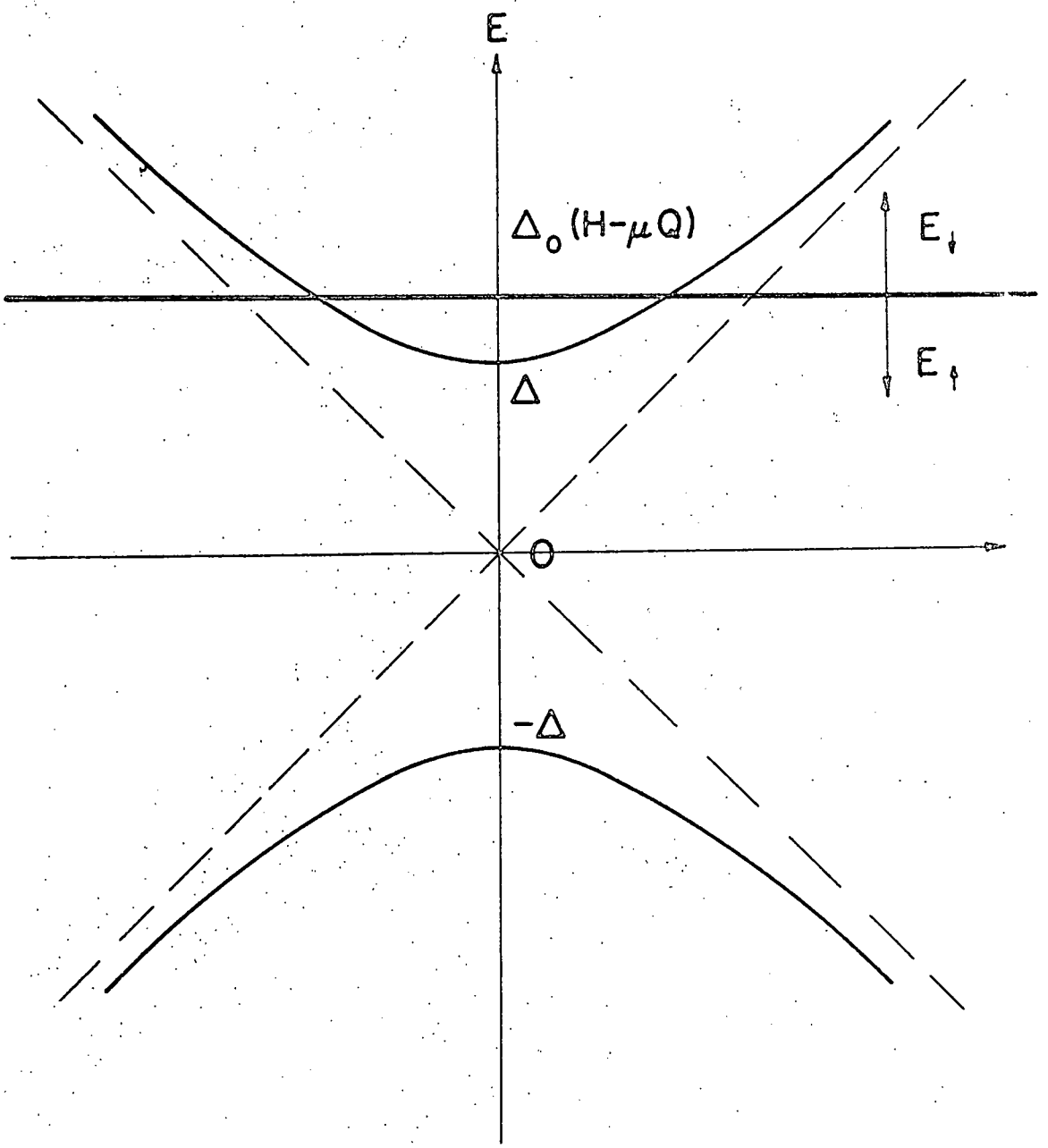

FIG. 9

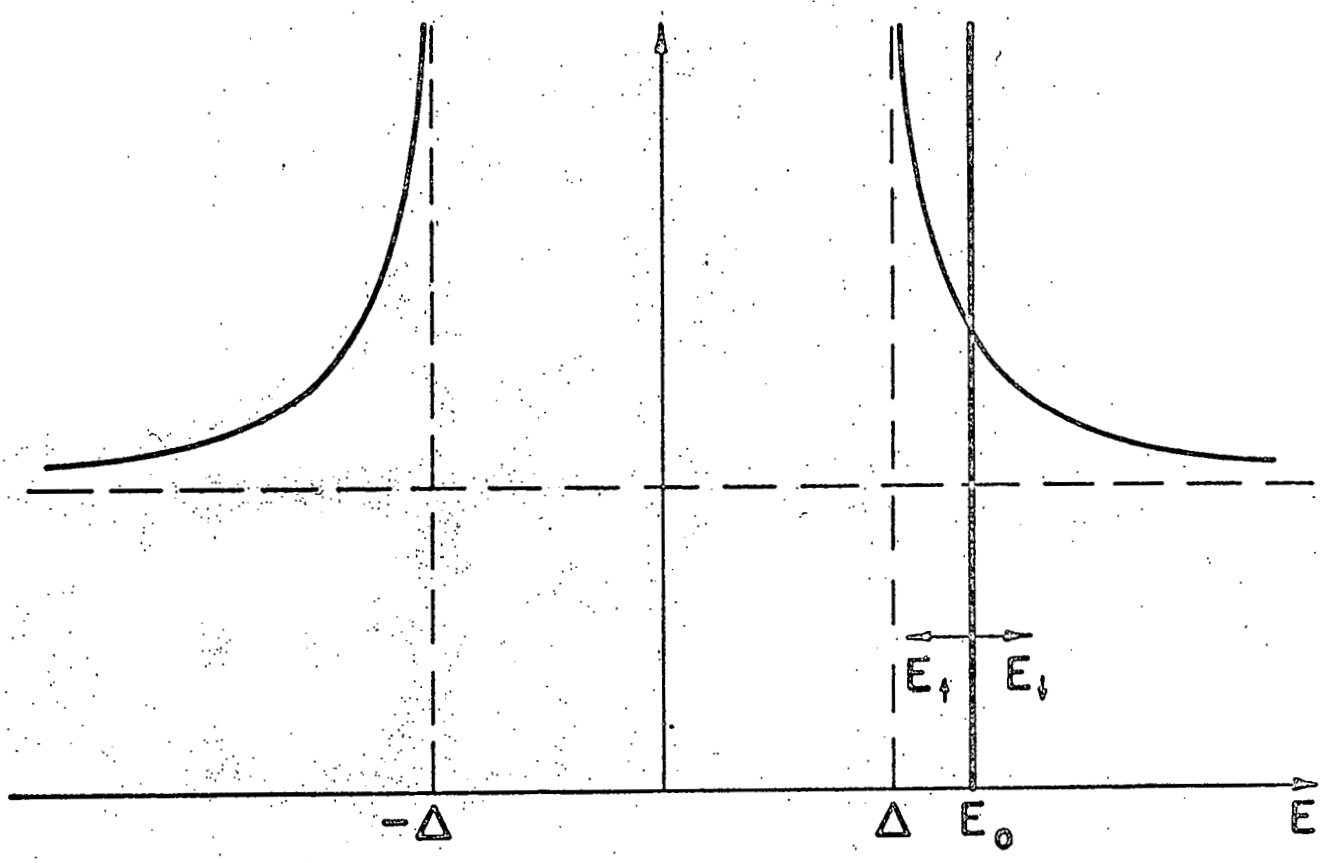

FIG. 10

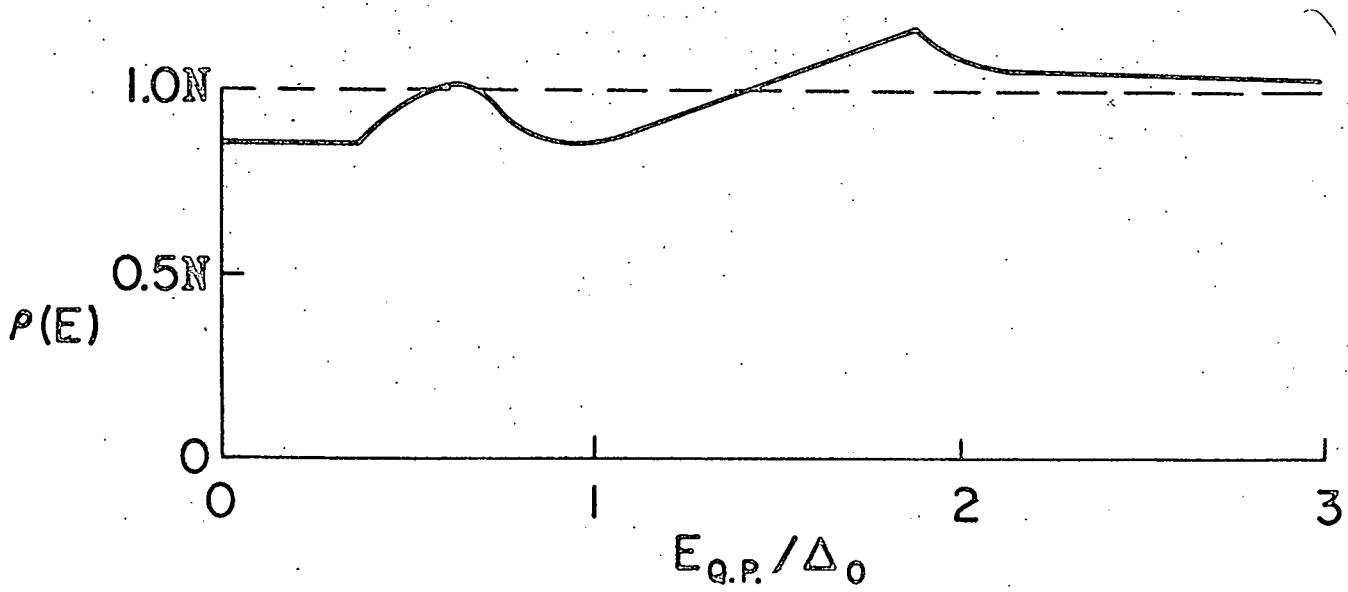

FIG. 11